Nucleophilic Displacement Reactions of *cis*-Bis((2,2′-biphenylylene)phosphochloridite ester)tetracarbonylmolybdenum(0). The First Example of an Unusual Hydrolysis Reaction Yielding Unsymmetrically Substituted Products

Houston Byrd,*,† Jeremiah D. Harden,† Jennifer M. Butler,‡ Michael J. Jablonsky,‡ and Gary M. Gray*,‡

Department of Biology, Chemistry & Mathematics, The University of Montevallo, Station 6480, Montevallo, Alabama 35115, and Department of Chemistry, The University of Alabama at Birmingham, 201 Chemistry Building, 1530 3rd Avenue South, Birmingham, Alabama 35204-1240

Received June 2, 2003

Ligands containing groups derived from bis(aryl)diols are widely used in asymmetric catalysis; however, few studies of the conformations of these ligands in transition-metal complexes have been reported. In this paper, the nucleophilic displacement reactions of *cis*-$Mo(CO)_4(2,2'\text{-}C_{12}H_8O_2PCl)_2$ (**1**) have been used to prepare a variety of complexes with [1,3,2]-dioxaphosphepin ligands, and the conformations of these ligands have been studied by NMR spectroscopy and X-ray crystallography. The nucleophilic substitution reactions yield both the expected disubstituted complexes *cis*-$Mo(CO)_4(2,2'\text{-}C_{12}H_8O_2PXR)_2$ (XR = NPr^n (**2**), OMe (**4**), SC_6H_4-4-Me (**6**)) and the unexpected hydrolysis products $[R'_3NH][cis\text{-}Mo(CO)_4(2,2'\text{-}C_{12}H_8O_2PO)(2,2'\text{-}C_{12}H_8O_2PXR)]$ ($R'_3 = Pr^nH_2$, XR = NPr^n, **3**; $R'_3 = Et_3$; XR = OMe, **5**). NMR studies have demonstrated that the hydrolysis product is the major product when more than a minute amount of water is present, even in the presence of a large excess of the nucleophiles. This reaction is complete in approximately 90 min at 25 °C. A very surprising feature of this reaction is that substitution of one chloride in **1** by the RX^- nucleophile greatly enhances the rate of substitution of the second chloride either by water or by another RX^- nucleophile. NMR studies of the [1,3,2]dioxaphosphepin complexes in chloroform-*d* solution suggest that the *R** and *S** enantiomers of the ligands interconvert via a low-energy pathway. Crystal structures of the complexes demonstrate that both the *R***S** diastereomer (**1**) and racemic mixtures of the *R***R** and *S***S** diastereomers (**2**−**4**) are observed in the solid state. These results suggest that bulkier biaryl groups are needed to prevent the racemization of the [1,3,2]dioxaphosphepin ligands in solution.

Introduction

A number of ligands containing [1,3,2]dioxaphosphepin groups (Figure 1) derived from bis(aryl)diols such as 2,2′-biphenol are currently used in asymmetric catalysis. Such ligands include symmetrical bis([1,3,2]-dioxaphosphepin) ligands,[1−3] asymmetrical bidentate phosphine−[1,3,2]dioxaphosphepin ligands,[4,5] and monodentate [1,3,2]dioxaphosphepin ligands.[6] The axially chiral diaryl backbone in the [1,3,2]dioxaphosphepin groups should result in C_2 symmetry at the phosphorus; however, recent studies of ligands containing [1,3,2]-dioxaphosphepin groups derived from 2,2′-biphenol suggested that there is a low-energy pathway to inversion of the biphenyl group, even when the ligand is coordinated to an inert metal center.[7] This suggests that the rational design of [1,3,2]dioxaphosphepin ligands for asymmetric catalysts requires a better understanding of the factors that affect the conformations of [1,3,2]-dioxaphosphepin groups.

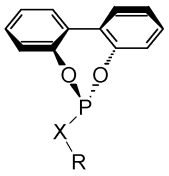

Figure 1. General structure of a [1,3,2]dioxaphosphepin ligand derived from bis(aryl)diols such as 2,2′-biphenol.

* To whom correspondence should be addressed. E-mail: gmgray@uab.edu (G.M.G.); byrdh@montevallo.edu (H.B.).
† The University of Montevallo.
‡ The University of Alabama at Birmingham.

(1) Hariharasarma, M.; Watkins, C. L.; Gray, G. M. *Organometallics* **2000**, *19*, 1232 and references therein.
(2) Billig, E.; Abatjoglou, A. G.; Bryant, D. R. (UCC) U.S. Patent 4,769,498, 1988.
(3) (a) Cuny, G. D.; Buchwald, S. L. *J. Am. Chem. Soc.* **1993**, *115*, 2066. (b) Johnson, J. R.; Cuny, G. D.; Buchwald, S. L. *Angew. Chem., Int. Ed. Engl.* **1995**, *34*, 1760.
(4) (a) Deerenberg, S.; Kamer, P. C. J.; van Leeuwen, P. W. N. M. *Organometallics* **2000**, *19*, 2065. (b) Suárez, A.; Méndez-Rojas, M. A.; Pizzano, A. *Organometallics* **2002**, *21*, 4611.
(5) (a) Sakai, N.; Mano, S.; Nozaki, K.; Takaya, H. *J. Am. Chem. Soc.* **1993**, *115*, 7033. (b) Nozaki, K.; Ojima, I. *Catalytic Asymmetric Synthesis*; Ojima, I., Ed.; Wiley-VCH: New York, 2000; Chapter 7.
(6) Reetz, M. T.; Mehler, G. *Angew. Chem., Int. Ed.* **2000**, *39*, 3889.
(7) Hariharasarma, M.; Lake, C. H.; Watkins, C. L.; Gray, G. M. *Organometallics* **1999**, *18*, 2593 and references therein.

10.1021/om030411z CCC: $25.00
Publication on Web 08/29/2003

There have been few studies of the conformations of [1,3,2]dioxaphosphepin ligands in transition-metal complexes, in large part because relatively few of these ligands have been prepared.[7] It should be possible to prepare complexes of [1,3,2]dioxaphosphepin ligands with a variety of functional groups using the nucleophilic displacement reactions of transition-metal-coordinated 2-chloro-[1,3,2]dioxaphosphepin ligands. Such reactions with chlorophosphines[8−17] and chlorophosphites derived from aliphatic diols[18−20] are a versatile method for the formation of complexes with unusual phosphorus-donor ligands. The coordination of the ligand to the transition metal stabilizes the phosphorus(III) oxidation state while maintaining a reactive phosphorus center. This allows the introduction of functional groups that are often unstable in the free ligands.

The structural characterization of a series of complexes of [1,3,2]dioxaphosphepin ligands would also be of aid in the development of databases for computational organometallic chemistry. Cundari has recently been computationally modeling the cone angle effects of phosphine ligands[21] that were initially empirically measured by Tolman.[22] However, his modeling was less successful for phosphites, due to the difficulty in accurately describing the P−O bonds. Additional structural data for phosphite complexes could lead to better modeling of the steric effects in these complexes.

Because of the wide applications of [1,3,2]dioxaphosphepin ligands in catalysis and the need for accurate data for computational studies, we have begun to prepare and structurally characterize transition-metal complexes with a variety of [1,3,2]dioxaphosphepin ligands. In this paper, we describe the synthesis (Figure 2) of the tetracarbonylmolybdenum(0) complex of (2,2′-biphenylylene)phosphochloridite ester, $Mo(CO)_4(2,2'\text{-}C_{12}H_8O_2PCl)_2$ (**1**), and nucleophilic displacement reactions of the chlorides in this complex by N-, O-, and S-nucleophiles. The solution conformations of the products have been characterized by multinuclear NMR spectroscopy, and the solid-state conformations of **1** and of three of the substitution products have been determined. The cis coordination of the [1,3,2]dioxaphosphepin ligands in **1** allows for interesting noncovalent interactions, and the rates of the chloride substitution reactions provide insight into the effect of the phosphite backbone.[20]

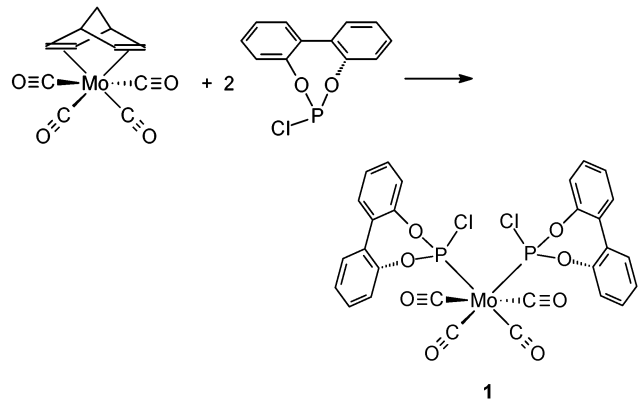

Figure 2. Reaction scheme for the formation of *cis*-$Mo(CO)_4(2,2'\text{-}C_{12}H_8O_2PCl)_2$.

Experimental Section

All reactions and purifications were carried out under high-purity nitrogen. All starting materials were reagent grade and were purified by sublimation or distillation before use. All solvents were dried and distilled immediately prior to use. Tetrahydrofuran (THF) and triethylamine were distilled from sodium/benzophenone under high-purity nitrogen. Hexanes were distilled from calcium hydride under high-purity nitrogen. Deuterated NMR solvents (chloroform-*d*, dichloromethane-d_2) were opened and stored under a nitrogen atmosphere at all times. *cis*-$Mo(CO)_4$nbd and 2,2′-biphenylylenephosphochloridite ester were synthesized using literature procedures.[23,24]

All one-dimensional $^{31}P\{^1H\}$, $^{13}C\{^1H\}$, and ^1H NMR spectra of the compounds were recorded using a Bruker ARX-300 NMR spectrometer with a quad (^1H, ^{13}C, ^{19}F, ^{31}P) 5 mm probe. The $^{31}P\{^1H\}$ NMR spectra were referenced to external 85% phosphoric acid, and both the ^{13}C and the ^1H NMR spectra were referenced to internal TMS. Two-dimensional $^1H-^1H$ Cosy-45, $^{13}C\{^1H\}$ HMBC, and $^{13}C\{^1H\}$ HMQC spectra were recorded using a Bruker DRX-400 NMR spectrometer. Biphenoxy rings were equivalent in all disubstituted complexes and are numbered so that the carbon bonded to oxygen is C1 and the bridging carbon is C6.

Elemental analyses were performed by Atlantic Microlabs, Norcross, GA. A solvent of crystallization is included in the calculated analysis only if the solvent was observed in the ^1H NMR spectrum of the analytical sample.

IR spectra of these complexes were performed on a Nicolet Nexus 470 FT-IR spectrometer. The compounds were dissolved in ethyl acetate (0.05 g/mL), and 5−6 drops were placed on a NaCl plate. The ethyl acetate was evaporated by blowing N_2 over the plate, leaving a film of the compound. The IR spectra of these films were taken at 4 cm^{-1} resolution and 16 scans.

***cis*-$Mo(CO)_4(2,2'\text{-}C_{12}H_8O_2PCl)_2$ (1).** A solution of 3.77 g (15.1 mmol) of 2,2′-biphenylylenephosphochloridite ester, 2.26 g (7.53 mmol) of $Mo(CO)_4$nbd, and 50 mL of dry hexanes in a Schlenk flask was stirred at room temperature overnight, during which time a white solid slowly precipitated from the solution. The solution was cooled to −5 °C for several hours, and then the precipitate was collected, washed with hexanes, and placed under high vacuum at room temperature overnight. This procedure produced 5.14 g (96.7%) of crude **1**. The crude **1** was purified by recrystallization from a dichloromethane/hexanes mixture to give analytically pure **1** as colorless crystals. Anal. Calcd for $C_{28}H_{16}Cl_2O_8P_2Mo$: C, 47.42; H, 2.28. Found: C, 47.48; H, 2.22. $^{31}P\{^1H\}$ NMR (chloroform-*d*): δ 192.45 (s). $^{13}C\{^1H\}$ NMR (carbonyl and aromatic carbons,

(8) Kraihanzel, C. S. *J. Organomet. Chem.* **1974**, *73*, 137 and references therein.
(9) Johanssen, G.; Stelzer, O.; Unger, E. *Chem. Ber.* **1975**, *108*, 1259.
(10) Ledner, P. W.; Beck, W.; Theil, G. *Inorg. Chim. Acta* **1976**, *20*, L11.
(11) Gray, G. M.; Kraihanzel, C. S. *J. Organomet. Chem.* **1978**, *146*, 23.
(12) Gray, G. M.; Kraihanzel, C. S. *J. Organomet. Chem.* **1980**, *187*, 51.
(13) Noth, H.; Reith, H.; Thorn, V. *J. Organomet. Chem.* **1978**, *159*, 165.
(14) Lindner, E.; Wuhrmann, J. C. *Chem. Ber.* **1981**, *114*, 2272.
(15) Wong, E. H.; Bradley, F. C. *Inorg. Chem.* **1981**, *20*, 2333.
(16) Treichel, P. M.; Rosenheim, L. D. *Inorg. Chem.* **1981**, *20*, 1539.
(17) Gray, G. M. *Inorg. Chim. Acta* **1984**, *81*, 157.
(18) Bartish, C. M.; Kraihanzel, C. S. *Inorg. Chem.* **1973**, *12*, 391.
(19) Gray, G. M.; Box, J. W.; Whitten, J. E. *Inorg. Chim. Acta* **1986**, *116*, 21.
(20) Gray, G. M.; Box, J. W.; Whitten, J. E. *Inorg. Chim. Acta* **1986**, *120*, 25.
(21) Cooney, K. D.; Cundari, T. R.; Hoffman, N. W.; Pittard, K. A.; Temple, M. D.; Zaho, T. *J. Am. Chem. Soc.*, in press.
(22) Tolman, C. A. *Chem. Rev.* **1977**, *77*, 313.
(23) Ehrl, W.; Ruck, R.; Vahrenkamp, H. *J. Organomet. Chem.* **1973**, *56*, 285.
(24) Verizhnikov, L. V.; Kirpichnikov, P. A. *Zh. Obshch. Khim.* **1966**, *37*, 1355.

chloroform-*d*): δ 209.53 (trans *C*O, aq, $|^2J(PC) + {}^2J(P'C)| =$ 41 Hz), 204.81 (cis *C*O, t, $|^2J(PC)| = 13$ Hz), 149.71 (aq, C1, $|^2J(PC) + {}^4J(P'C)| = 11$ Hz), 122.85 (bs, C2), 126.84 (s, C3,), 129.93 (s, C4), 130.64 (s, C5), 130.57 (s, C6). ^{1}H NMR (aromatic carbons, chloroform-*d*): δ 7.16 (bdd, H2, $|^3J(HH)| = 8$ Hz, $|^4J(HH)| = 2$ Hz), 7.28 (bddd, H3, $|^3J(HH)| = |^3J(HH)| = 8$ Hz, $|^4J(HH)| = 2$ Hz), 7.34 (ddd, H4, $|^3J(HH)| = |^3J(HH)| = 8$ Hz, $|^4J(HH)| = 2$ Hz), 7.45 (dd, H5, $|^3J(HH)| = 8$ Hz, $|^4J(HH)| = 2$ Hz). IR: ν_{CO} (cm^{-1}) 2055 (s), 1975 (sh) 1947 (s).

***cis*-Mo(CO)$_4$(2,2′-C$_{12}$H$_8$O$_2$PNHCH$_2$CH$_2$CH$_3$)$_2$ (2) and [CH$_3$CH$_2$CH$_2$NH$_3$] [*cis*-Mo(CO)$_4$(2,2′-C$_{12}$H$_8$O$_2$PNHCH$_2$CH$_2$CH$_3$)(2,2′-C$_{12}$H$_8$O$_2$PO)] (3).** Excess *n*-propylamine (2.0 mL), which had been distilled from KOH, was added via cannula transfer to a solution of 0.50 g (0.71 mmol) of **1** in 10 mL of dry THF. The mixture was stirred at room temperature over the weekend and then was filtered to remove the *n*-propylammonium chloride. The solution was rotary evaporated to dryness, leaving a white solid. The solid was stirred in hot hexanes overnight to completely separate compound **2** (soluble) from compound **3** (insoluble) and then filtered. The filtrate was evaporated to dryness to yield 0.27 g (51%) of crude **2**. The hexanes-insoluble solid was washed with hexanes and dried under vacuum to yield 0.081 g (15%) of crude **3**.

The crude **2** was purified by recrystallization from a dichloromethane/hexanes mixture to give analytically pure **2** as colorless crystals. Anal. Calcd for $C_{34}H_{32}N_2O_8P_2Mo$: C, 54.12; H, 4.27; N, 3.71. Found: C, 54.17; H, 4.24; N, 3.66. ^{31}P{^{1}H} NMR (chloroform-*d*): δ 175.71 (s). ^{13}C{^{1}H} NMR (carbonyl, aromatic and aliphatic carbons, chloroform-*d*): δ 210.82 (trans *C*O, aq, $|^2J(PC) + {}^2J(P'C)| = 27$ Hz), 206.33 (cis *C*O, t, $|^2J(PC)| = 13$ Hz), 149.83 (aq, C1, $|^2J(PC) + {}^4J(P'C)| = 9$ Hz), 121.28 (s, C2), 124.15 (s, C3,), 128.24 (s, C4), 128.77 (s, C5), 129.37 (s, C6), 42.63 (s, *C*H$_2$), 24.10 (s, *C*H$_2$) 9.89 (s, *C*H$_3$). ^{1}H NMR (chloroform-*d*): δ 7.18−7.44 (m, 16H, Ar), 3.57 (m, 2H, NH), 2.59 (m, 4H, NHC*H*$_2$) 1.24 (tq, 4H, C*H*$_2$CH$_3$, $|^3J(HH)| = |^3J(HH)| = 7$ Hz)), 0.64 (t, 6H, CH$_3$, $|^3J(HH)| = 7$ Hz). IR: ν_{CO} (cm^{-1}) 2036 (s), 1943 (sh), 1918 (s).

The crude **3** was purified by recrystallization from a dichloromethane/hexanes mixture to give analytically pure **3** as colorless crystals. Anal. Calcd for $C_{34}H_{34}N_2O_9P_2Mo$: C, 52.29; H, 4.19; N, 3.63. Found: C, 52.46; H, 4.47; N, 3.70. ^{31}P{^{1}H} NMR (chloroform-*d*): δ 175.97 (d, *P*N, $|^2J(PP)| = 43$ Hz), 165.61 (d, *P*O$^-$, $|^2J(PP)| = 43$ Hz). ^{1}H NMR (chloroform-*d*): δ 7.23−7.50 (m, 16H, Ar), 2.52 (M, 2H, NHC*H*$_2$), 2.24 (m, 2H, NH$_2$C*H*$_2$), 1.35 (m, 2H, CH$_2$CH$_3$), 1.18 (m, 2H, CH$_2$CH$_3$), 0.67 (t, 3H, CH$_3$, $|^3J(HH)| = 7$ Hz), 0.61 (t, 3H, CH$_3$, $|^3J(HH)| = 7$ Hz). IR: ν_{CO} (cm^{-1}) 2022 (s), 1924 (sh), 1900 (s).

***cis*-Mo(CO)$_4$(2,2′-C$_{12}$H$_8$O$_2$POCH$_3$)$_2$ (4) and [(C$_2$H$_5$)$_3$NH][*cis*-Mo(CO)$_4$(2,2′-C$_{12}$H$_8$O$_2$POCH$_3$)(2,2′-C$_{12}$H$_8$O$_2$PO)] (5).** A mixture of 3.0 mL of methanol and 2.0 mL of triethylamine was added via cannula transfer to a solution of 0.50 g (0.71 mmol) of **1** in 10 mL of dry THF. The mixture was stirred at room temperature overnight and then was filtered to remove the triethylammonium chloride precipitate. The filtrate was evaporated to dryness to yield a white solid residue. The solid was stirred in hot hexanes overnight to completely separate compound **4** (soluble) from compound **5** (insoluble) and then filtered. The filtrate was evaporated to dryness to yield 0.40 g (81%) of crude **4**. The hexanes-insoluble solid was washed with hexanes and dried under high vacuum to yield 0.069 g (12%) of crude **5**.

The crude **4** was purified by recrystallization from a dichloromethane/hexanes mixture to give analytically pure **4** as colorless crystals. Anal. Calcd for $C_{30}H_{22}O_{10}P_2Mo$: C, 51.48; H, 3.14. Found: C, 51.36; H, 3.43. ^{31}P{^{1}H} NMR (chloroform-*d*): δ 173.04 (s). ^{13}C{^{1}H} NMR (carbonyl, aromatic, and aliphatic carbons, chloroform-*d*): δ 209.80 (trans *C*O, aq, $|^2J(PC) + {}^2J(P'C)| = 33$ Hz), 205.23 (cis *C*O, t, $|^2J(PC)| = 14$ Hz), 148.83 (aq, C1, $|^2J(PC) + {}^4J(P'C)| = 9$ Hz), 121.11 (s, C2), 124.40 (s, C3), 128.36 (s, C4), 129.03 (s, C5), 127.25 (s, C6), 53.17 (aqueous *C*H$_3$, $|^2J(PC) + {}^4J(P'C)| = 8$ Hz). ^{1}H NMR (chloroform-*d*): δ 7.17−7.40 (m, 16H, Ar), 3.54 (aq, 6H, CH$_3$, $|^3J(PH) + {}^5J(P'H)| = 7$ Hz). IR: ν_{CO} (cm^{-1}) 2027 (s), 1929 (sh), 1910 (s).

The crude **5** was purified by recrystallization from a dichloromethane/hexanes mixture to give analytically pure **5** as a white powder. Anal. Calcd for $C_{35}H_{35}NO_{10}P_2Mo$: C, 53.37; H, 4.49; N, 1.78. Found: C, 53.21; H, 4.54; N, 1.81. ^{31}P{^{1}H} NMR (chloroform-*d*): δ 179.02 (d, *P*OCH$_3$, $|^2J(PP)| = 51$ Hz), 160.20 (d, *P*O$^-$, $|^2J(PP)| = 51$ Hz). ^{1}H NMR (chloroform-*d*): δ 7.00−7.54 (m, 16H, Ar), 3.59 (d, 3H, OC*H*$_3$, $|^2J(PH)| = 11$ Hz), 2.61 (q, 6H, NC*H*$_2$, $|^3J(HH)| = 7$ Hz), 0.929 (t, 9H, CH$_3$, $|^3J(HH)| = 7$ Hz).

***cis*-Mo(CO)$_4${2,2′-C$_{12}$H$_8$O$_2$PSC$_6$H$_4$-4-CH$_3$}$_2$ (6).** A solution of 0.15 g (1.4 mmol) of dry thiocresol in 10 mL of THF was added via cannula transfer to a solution of 0.50 g (0.71 mmol) of **1** in 10 mL of dry THF. Next, 2.0 mL of dry triethylamine was added via cannula transfer. The mixture was stirred at room temperature overnight and then filtered to remove the triethylammonium chloride precipitate. The filtrate was evaporated to dryness, and the white solid residue was stirred in hot hexanes overnight. The insoluble portion of the solid was removed by filtration, and the filtrate was evaporated to dryness to yield 0.13 g (21%) of crude **6**. The crude **6** was purified by recrystallization from a dichloromethane/hexanes mixture to give analytically pure **6** as a white solid. Anal. Calcd for $C_{42}H_{30}O_8P_2S_2Mo$: C, 57.01; H, 3.42. Found: C, 57.16; H, 3.48. ^{31}P{^{1}H} NMR (chloroform-*d*): δ 213.29 (s). ^{13}C{^{1}H} NMR (carbonyl, chloroform-*d*): δ 213.12 (trans *C*O, aqueous, $|^2J(PC) + {}^2J(P'C)| = 35$ Hz), 207.55 (cis *C*O, t, $|^2J(PC)| = 12$ Hz). ^{1}H NMR (chloroform-*d*): δ 6.80−7.40 (m, 24H, Ar), 2.23 (s, 6H, CH$_3$).

^{31}P{^{1}H} NMR Studies of the Reaction of 1 with *n*-Propylamine. A 0.028 M solution of **1** in tetrahydrofuran-d_8 was prepared in an NMR tube, and its ^{31}P{^{1}H} NMR spectrum was taken. Then, a 2.5-fold excess of *n*-propylamine was added to the NMR tube, and NMR spectra were taken at intervals until the ^{31}P NMR resonance of **1** had disappeared. The NMR temperature was 298 K.

X-ray Data Collection and Solution. Suitable single crystals of **1**−**4** were mounted on glass fibers with epoxy cement and aligned upon an Enraf-Nonius CAD4 single-crystal diffractometer under aerobic conditions. Standard peak search and automatic indexing routines followed by least-squares fits of 25 accurately centered reflections resulted in accurate unit cell parameters. The space groups of the crystals were assigned on the basis of systematic absences and intensity statistics. All data collection was carried out using the CAD4-PC software,[25] and details of the data collections are given in Table 1. The analytical scattering factors of the complex were corrected for both $\Delta f'$ and $i\Delta f''$ components of anomalous dispersion. All data were corrected for the effects of absorption and for Lorentz and polarization effects.

All crystallographic calculations were performed with the Siemens SHELXTL-PC program package.[26] The Mo and P positions were located using the Patterson method and the remainder of the non-hydrogen atoms was located in difference Fourier maps. Full-matrix refinement of the positional and anisotropic thermal parameters for all non-hydrogen atoms versus F^2 was carried out. All hydrogen atoms were placed in calculated positions with the appropriate molecular geometry and d(C−H) = 0.96 Å. The isotropic thermal parameter associated with each hydrogen atom was fixed equal to 1.2 times the U_{eq} value of the atom to which it was bound. The correct enantiomer for **1** was chosen on the basis of its Flack parameter. Selected bond lengths for complexes **1**−**4** are given in Table 2, selected bond angles for complexes **1**−**4** are given

(25) CAD4-PC Version 1.2; Enraf-Nonius, Delft, The Netherlands, 1988.

(26) Sheldrick, G. M. SHELXTL NT version 5.10; Bruker AXS, Madison, WI, 1999.

Table 1. Experimental Data of Crystallographic Studies of Compounds 1−4

	1	2	3	4
formula	$C_{28}H_{16}Cl_2MoO_8P_2$	$C_{34}H_{32}MoN_2O_8P_2$	$C_{34}H_{34}MoN_2O_9P_2$	$C_{30}H_{22}MoO_{10}P_2$
mol wt	709.19	754.50	772.51	700.36
space group	$P2_12_12_1$	$P\bar{1}$	$P\bar{1}$	$P2_1/n$
a (Å)	12.258(3)	10.586(2)	10.765(2)	8.6520(17)
b (Å)	13.050(3)	13.129(3)	12.138(2)	18.725(4)
c (Å)	18.478(4)	13.309(3)	15.511(3)	19.165(4)
α (deg)	90	78.87(3)	91.91(3)	90
β (deg)	90	67.79(3)	103.86(3)	100.45(3)
γ (deg)	90	81.41(3)	114.31(3)	90
Z	4	2	2	4
d_{calcd} (g/cm^3)	1.594	1.496	1.447	1.523
h_{max}, h_{min}	0, 13	−11, 11	−10, 11	−9, 9
k_{max}, k_{min}	−1, 14	−14, 1	−13, 1	−20, 0
l_{max}, l_{min}	−19, 0	14, 14	−16, 16	−1, 20
2θ limits (deg)	1.91−22.46	2.09−22.47	2.14−22.48	2.16−22.47
no. of rflns measd	2391	5054	5416	4409
no. of indep rflns measd	2359	4360	4624	3983
R_{int} (%)	2.54	2.13	3.96	4.06
scan type	$\omega-2\theta$	$\omega-2\theta$	$\omega-2\theta$	$\omega-2\theta$
abs cor	none	empirical	empirical	none
abs coeff (mm^{-1})	0.781	0.541	0.515	0.590
no. of variables	371	435	437	391
extinction coeff	0.0055(3)	0.0202(10)	0.0004(4)	0.0015(2)
R, %	3.14 (2σ)	3.08 (2σ)	4.35 (2σ)	5.11 (2σ)
R_w, %	7.17 (2σ)	7.91 (2σ)	10.58 (2σ)	10.46 (2σ)
GOF	1.073	1.106	1.042	0.990

Table 2. Selected Bond Distances (Å) with Their Esds for Compounds 1−4

	1	2	3	4
Mo−P1	2.406(2)	2.4610(11)	2.4670(18)	2.444(2)
Mo−P2	2.4048(19)	2.4671(12)	2.4460(17)	2.432(2)
X−P1	2.059(3)	1.617(4)	1.513(4)	1.575(5)
X−P2	2.056(3)	1.631(3)	1.638(5)	1.591(7)
O1−P1	1.614(5)	1.632(2)	1.664(4)	1.622(5)
O2−P1	1.595(5)	1.643(2)	1.652(4)	1.613(5)
O3−P2	1.621(5)	1.635(2)	1.634(4)	1.592(5)
O4−P2	1.602(5)	1.633(2)	1.639(4)	1.624(6)
C25−Mo	2.006(9)	2.018(4)	1.988(8)	1.132(9)
C26−Mo	2.030(9)	2.005(4)	1.976(7)	1.997(10)
C27−Mo	2.071(9)	2.040(4)	1.995(8)	2.028(9)
C28−Mo	2.048(9)	2.024(4)	2.050(8)	2.027(8)
C25−O5	1.134(10)	1.135(4)	1.155(8)	1.132(9)
C26−O6	1.134(9)	1.131(4)	1.156(7)	1.152(9)
C27−O7	1.131(9)	1.140(4)	1.153(8)	1.137(9)
C28−O8	1.173(10)	1.143(4)	1.128(7)	1.133(8)

Table 3. Selected Bond Angles (deg) with Their Esds for Compounds 1−4

	1	2	3	4
C25−Mo−C26	90.5(4)	89.60(15)	86.6(3)	90.7(3)
C25−Mo−C27	89.3(4)	85.62(14)	91.1(3)	90.8(3)
C25−Mo−C28	91.0(4)	85.36(14)	92.6(3)	91.2(3)
C26−Mo−C27	89.9(4)	92.38(15)	93.0(3)	88.2(3)
C26−Mo−C28	90.3(4)	87.79(14)	93.2(3)	88.5(3)
C27−Mo−C28	179.6(4)	170.97(13)	172.9(3)	176.2(4)
C25−Mo−P1	179.3(3)	175.43(10)	170.93(18)	176.4(2)
C25−Mo−P2	91.5(3)	89.58(10)	91.00(18)	89.2(2)
C26−Mo−P1	88.8(2)	85.94(11)	84.6(2)	92.9(3)
C26−Mo−P2	174.9(3)	177.26(11)	177.4(2)	177.5(2)
C27−Mo−P1	90.7(2)	93.60(11)	91.6(2)	89.0(2)
C27−Mo−P2	85.4(2)	90.17(11)	88.05(19)	94.3(3)
C28−Mo−P1	89.0(2)	95.42(10)	85.7(2)	89.2(2)
C28−Mo−P2	94.4(3)	89.54(10)	85.83(19)	89.0(2)
P1−Mo−P2	89.23(7)	94.93(4)	97.74(6)	87.23(8)

in Table 3, and selected torsion angles for complexes **1**−**4** are given in Table 4.

Results and Discussion

Synthesis of *cis*-Mo(CO)$_4$(2,2′-C$_{12}$H$_8$O$_2$PCl)$_2$ (1). The reaction scheme for the preparation of **1** is shown

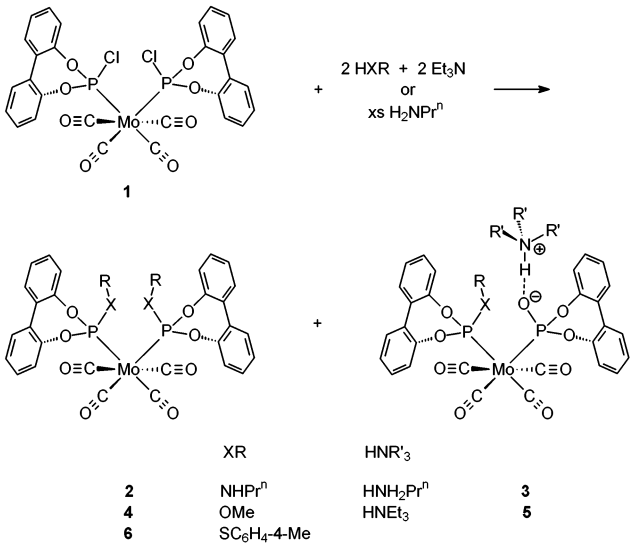

Figure 3. Reaction scheme for the nucleophilic substitution reactions. All reactions were carried out at room temperature in dry THF with dry triethylamine or propylamine as a base.

Table 4. Selected Torsion Angles (deg) and Their Esds for Compounds 1−4

	1	2	3	4
C6−C1−O1−P1	−75.3(7)	78.1(3)	70.5(6)	73.9(9)
C7−C12−O2−P1	−73.7(8)	72.3(4)	81.4(6)	70.19(9)
C18−C13−O3−P2	73.6(8)	74.6(3)	75.8(6)	72.2(9)
C19−C24−O4−P2	67.8(9)	74.3(3)	78.1(6)	75.9(9)
P1−Mo−P2−X	152.41(12)	12.69(14)	6.4(2)	87.4(3)
P2−Mo−P1−X	−77.44(11)	98.19(17)	164.8(2)	83.5(3)

in Figure 2. The $^{31}P\{^1H\}$ NMR spectrum of the hexanes-insoluble product contained a single resonance at 192.45 ppm due to **1** and did not exhibit a resonance at 179.89 ppm that would have indicated the presence of unreacted free ligand of the product. The fact that a single, sharp ^{31}P NMR resonance is observed for **1** suggests that the diastereomers of the complex are interconverting rapidly at ambient temperature.

Nucleophilic Displacement Reactions of the Chloride Groups in 1. The general reaction scheme for the nucleophilic displacement reactions is shown in Figure 3. The starting material, **1**, was reacted with a stoichiometric amount of dry triethylamine and of the dried and purified nucleophile in dry THF, except when the nucleophile was *n*-propylamine, where only an excess of the *n*-propylamine was used.[27] Two products were observed for each reaction. In each case, the two products were readily separated, due to the fact that only the major product was soluble in hot hexanes. It should be noted that NMR studies indicate that these nucleophilic substitution reactions are complete after 90 min. They were typically set up to run overnight or over the weekend as a matter of convenience.

The assignments of the products were made on the basis of their $^{31}P\{^1H\}$ NMR spectra and were confirmed by elemental analyses. The major and expected product was one in which both chloride groups were displaced by the nucleophile. The $^{31}P\{^1H\}$ NMR resonances of these complexes are singlets due to the equivalent

(27) THF and triethylamine were dried over Na−benzophenone and were not used until a deep purple color was observed for at least 24 h. Propylamine was first placed over KOH for 24 h and then refluxed and distilled from CaH_2.

chemical environments of the phosphorus nuclei. The minor products were those in which one chloride group had been replaced by the nucleophile and the other chloride group had been replaced by a hydroxy group. The $^{31}P\{^1H\}$ NMR resonances of these complexes are two doublets, due to the inequivalent chemical environments of the phosphorus nuclei.

It was somewhat surprising that two products were obtained from these reactions, because previous reactions of similarly dried nucleophiles with the related complex *cis*-$Mo(CO)_4(Ph_2PCl)_2$ have not been observed to yield hydrolysis products.[11,12] This suggests that **1** is particularly susceptible to hydrolysis and that only very small amounts of water are required for hydrolysis to occur.

To better understand the unexpected formation of the hydrolysis products, the reactions of **1** with excesses of "dry"[27] and "wet"[28] *n*-propylamine were followed by $^{31}P\{^1H\}$ NMR spectroscopy. Selected NMR spectra for the reaction of **1** with "dry" *n*-propylamine are shown in Figure 4. The $^{31}P\{^1H\}$ NMR resonances of the hydrolysis product, **3** (doublets at 180.62 and 169.27 ppm), were observed first, apparently from residual water in the "dry" *n*-propylamine and tetrahydrofuran-d_8. The formation of **3** was completed after 10 min, and then the $^{31}P\{^1H\}$ NMR resonance of the disubstitution product, **2** (singlet at 183.27 ppm), began to appear. The disubstitution reaction was completed after 90 min. The amount of the hydrolysis product does not change during the formation of the disubstituted product, which suggests that the two products are formed by different mechanisms.

The reaction of **1** with "wet" *n*-propylamine was similar to that of **1** with "dry" *n*-propylamine. The hydrolysis product, **3**, was observed after 5 min, while the ^{31}P NMR resonance of the disubstitution product, **2**, did not appear until after 15 min. The major product was **3** (91% from integration of the $^{31}P\{^1H\}$ NMR resonances), although a ^1H NMR spectrum of the "wet" *n*-propylamine showed that less than 5% water was present in the "wet" *n*-propylamine. These spectra clearly indicate that the reaction to form the hydrolysis product, **3**, is significantly more rapid than is the reaction to form the disubstitution product, **2**, and that the products of the two reactions do not interconvert.

Small resonances due to a monosubstituted intermediate (doublet at 197.57 ppm partially obscured by the resonance of **1**; doublet at 180.43 ppm, $|^2J(PP')| = 44$ Hz) are observed in the $^{31}P\{^1H\}$ NMR spectra of both the "dry" and "wet" reaction mixtures. The chemical shifts of the $^{31}P\{^1H\}$ NMR resonances of the intermediate suggest that it is *cis*-$Mo(CO)_4(2,2'\text{-}C_{12}H_8O_2PNHPr^n)$-$(2,2'\text{-}C_{12}H_8O_2PCl)$. This is consistent with *n*-propylamine both being a better nucleophile and having a much higher concentration than the water.

The low concentration of the intermediate in each reaction and the observation that the intensities of both of the doublets **3** increase at the same rate suggests that the substitution of the chloride in the monosubstituted intermediate by either water or *n*-propylamine occurs significantly more rapidly than does the substitution of a chloride in **1** by *n*-propylamine. The more rapid reaction of the intermediate with water explains why the concentration of the intermediate is lower in the reaction with "wet" *n*-propylamine than in the reaction with "dry" *n*-propylamine. Additional studies will be needed to determine the mechanism that gives rise to the more rapid nucleophilic substitution reactions of the intermediate complex, but it seems likely that this will involve interactions between the 2-(*n*-propylamino)-1,3,2-dioxaphosphepin ligand and the incoming nucleophile and possibly with the adjacent 2-chloro-1,3,2-dioxaphosphephin ligand.

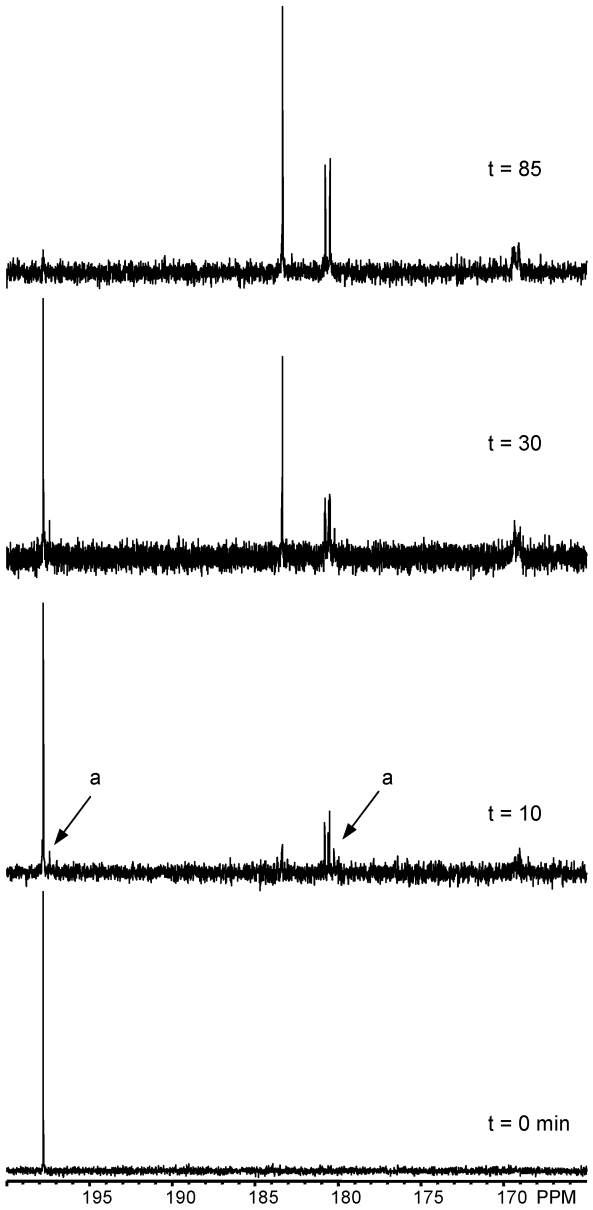

Figure 4. ^{31}P NMR of the reaction of *cis*-$Mo(CO)_4(2,2'\text{-}C_{12}H_8O_2PCl)_2$ (compound **1**) with "dry" propylamine. Spectra were taken at various timed intervals. The two doublets at 180.62 and 169.27 ppm are assigned to the hydrolysis product, compound **3**. The singlet at 183.27 ppm is assigned to the disubstituted propylamine, compound **2**. The arrows (a) indicate the formation of resonances due to the intermediate species. Both resonances disappear by the end of the reaction.

(28) *n*-Propylamine was used without drying. A ^1H NMR spectrum of *n*-propylamine in chloroform-*d* gave the expected integration for the four *n*-propylamine resonances (2:2:2:3), indicating that only a small amount of water (<5%) was present.

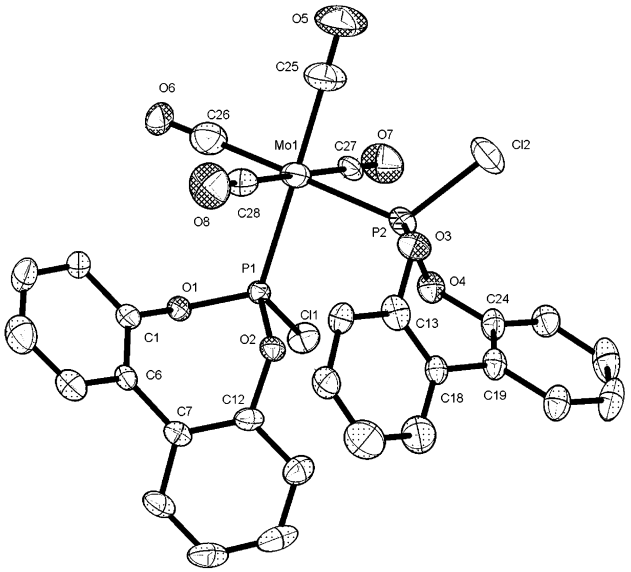

Figure 5. ORTEP drawing of the molecular structure of the major conformer of **1**. Thermal ellipsoids are drawn at the 25% probability level, and hydrogen atoms are omitted for clarity.

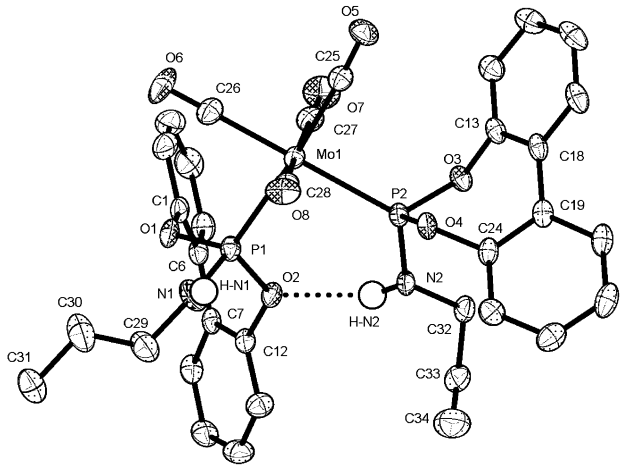

Figure 6. ORTEP drawing of the molecular structure of the major conformer of **2**. Thermal ellipsoids are drawn at the 25% probability level, and hydrogen atoms are omitted for clarity. Hydrogen bonding is shown by the dotted line.

NMR Spectroscopic Characterization of the Complexes. The chemical shifts of $^{13}C\{^1H\}$ NMR resonances and the magnitudes of the C−P coupling constants of the CO ligands are consistent with the [1,3,2]dioxaphosphepin ligands being oriented in a cis geometry. The $^{13}C\{^1H\}$ NMR resonances for the carbonyls cis to both [1,3,2]dioxaphosphepin ligands (*cis*-CO) are observed between 204 and 208 ppm. Each resonance is a triplet with $|^2J(PC)|$ between 12 and 14 Hz. The $^{13}C\{^1H\}$ NMR resonances of the carbonyls trans to one of the phosphepin ligands (trans-CO) are farther downfield between 209 and 213 ppm. Each of these resonances is an apparent quintet (A portion of an AXX′ spin system[29]) with a $|^2J(PC) + {}^2J(P'C)|$ value between 27 and 41 Hz.

The chemical shifts of the $^{31}P\{^1H\}$ NMR resonances of **1, 2, 4**, and **6** are extremely sensitive to the nature of the nucleophile that is bound to the P atom.[30,31] However, the chemical shift of the $^{31}P\{^1H\}$ NMR resonance does not appear to be related to the electronegativity of the heteroatom bound to the phosphorus. Similar trends in ^{31}P NMR chemical shifts of the [1,3,2]dioxaphosphorinane ligands in $Mo(CO)_5\{RXP(OCH_2CMe_2CH_2O)\}$ and $Mo(CO)_5\{RXP(OCH_2CH_2CHMeO)\}$ complexes have previously been observed, but not in the ^{31}P NMR chemical shifts of Ph_2PXR ligands in $Mo(CO)_5(Ph_2PXR)$ and *cis*-$Mo(CO)_4(Ph_2PXR)_2$ complexes.[19,20]

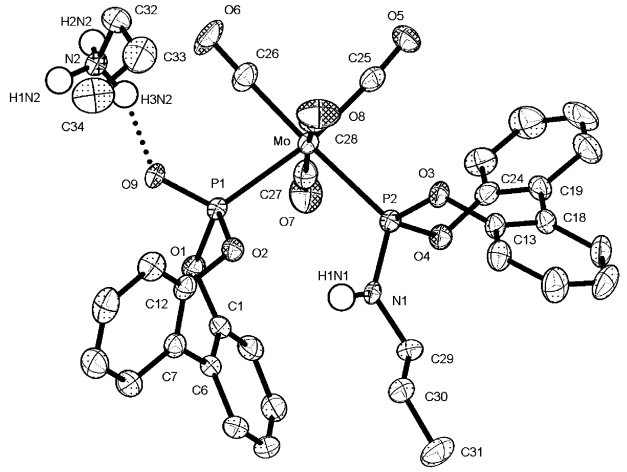

Figure 7. ORTEP drawing of the molecular structure of the major conformer of **3**. Thermal ellipsoids are drawn at the 25% probability level, and hydrogen atoms are omitted for clarity. Hydrogen bonding is shown by the dotted line.

Each of the disubstituted complexes, **1**, **2**, **4**, and **6**, exhibits a $^{31}P\{^1H\}$ NMR resonance that is a sharp singlet. This indicates either that only the *R**S** conformation is present in solution or that the *R** and *S** conformations[32] of the rings are rapidly interconverting in solution. The second explanation seems most likely on the basis of previous work[1] and because both *R**S** and *R**R**/*S**S** conformations are found in the solid-state conformations of the complexes.

All of the resonances of the carbons and hydrogens in **1** have been assigned using 2D NMR spectroscopy. A $^1H-^1H$ COSY-45 NMR experiment was run to determine the $^1H-^1H$ coupling, and the $^1H-^{13}C$ connectivity was determined using a $^1H\{^{13}C\}$ HMBC NMR experiment. $^1H\{^{13}C\}$ HMQC was used to assign protons to their respective carbons. For compounds **2** and **4**, the ^{13}C NMR spectra in the aromatic region are similar to that of **1**, and the assignment has been made in a consistent fashion. The ^1H NMR spectra of **2** and **4** in the aromatic region are less clearly defined, and no attempt has been made to assign the aromatic ^1H resonances of these complexes.

X-ray Crystal Structures for Compounds 1−4. The molecular structures of **1**−**4** have been determined and are shown in Figures 5−8, respectively. The coordination environment of the molybdenum in each complex is a slightly distorted octahedron. The distortion seems to be dictated by the position of the nucleophile (XR). For compounds **1** and **4**, the XR groups are

(29) Redfield, D. A.; Nelson, J. H.; Cary, L. W. *Inorg. Nucl. Chem. Lett.* **1974**, *10*, 727.

(30) Pregosin, P. S.; Kunz, R. W. *NMR Basic Princ. Prog.* **1979**, *16*, 47.

(31) Gorenstein, D. G. *Phosphorus-31 NMR, Principles and Applications*; Academic Press: New York, 1984; pp 7−8.

(32) Throughout this paper, *R** and *S** are used to refer to the relative conformations of the 2,2′-biphenyl groups. The first conformation referred to in a molecule is designated *R** by convention.

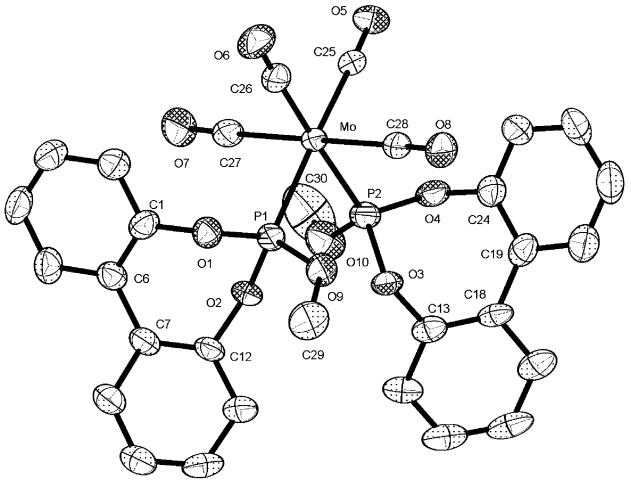

Figure 8. ORTEP drawing of the molecular structure of the major conformer of **4**. Thermal ellipsoids are drawn at the 25% probability level, and hydrogen atoms are omitted for clarity.

Table 5. Planes Used To Define the Seven-Membered Phosphepin Rings for Compounds 1−4

compd	space group	plane	angle	value, deg
1	$P2_12_12_1$	1. O1−P1−O2	1−2	59.1
		2. O1−C1−C6	1−3	51.1
		3. O2−C12−C7	2−3	47.7
		1: O3−P2−O4	1−2	55.8
		2: O3−C13−C18	1−3	51.1
		3: O4−C24−C19	2−3	45.2
2	$P\bar{1}$	1: O1−P1−O2	1−2	58.8
		2: O1−C1−C6	1−3	54.1
		3: O2−C12−C7	2−3	45.9
		1: O3−P2−O4	1−2	56.6
		2: O3−C13−C18	1−3	55.3
		3: O4−C24−C19	2−3	46.0
3	$P\bar{1}$	1: O1−P1−O2	1−2	54.4
		2: O1−C1−C6	1−3	62.4
		3: O2−C12−C7	2−3	48.5
		1: O3−P2−O4	1−2	57.5
		2: O3−C13−C18	1−3	60.3
		3: O4−C24−C19	2−3	47.4
4	$P2_1/n$	1: O1−P1−O2	1−2	57.0
		2: O1−C1−C6	1−3	53.7
		3: O2−C12−C7	2−3	47.0
		1: O3−P2−O4	1−2	55.4
		2: O3−C13−C18	1−3	58.8
		3: O4−C24−C19	2−3	46.8

oriented "outside" of the P1−Mo−P2 bite angle, and this angle is slightly less than 90°. In contrast, compounds **2** and **3** have one XR group oriented "inside" of the P1−Mo−P2 bite angle, and this angle is greater than 90° in both complexes. The orientations of the XR groups in **2** and **3** may be due to hydrogen bonding, although the hydrogen bonding in the two complexes is quite different. In **2**, hydrogen bonding between the amine proton of the *n*-propylamino group and one of the oxygens of the adjacent phosphepin ring is observed. In contrast, hydrogen bonding occurs between the ammonium proton of the *n*-propylammonium cation and the anionic phosphito oxygen in **3**.

The carbonyls trans to the phosphepin ligands in **1**−**4** have shorter Mo−C bonds than do the carbonyls trans to carbonyls. This is consistent with the phosphepin ligands being better σ-donors and/or poorer π-acceptors than the carbonyl ligands. However, there is no corresponding difference in the C−O bond lengths of the carbonyl ligands. These observations have been reported by a number of authors, and one example is given in ref 33.

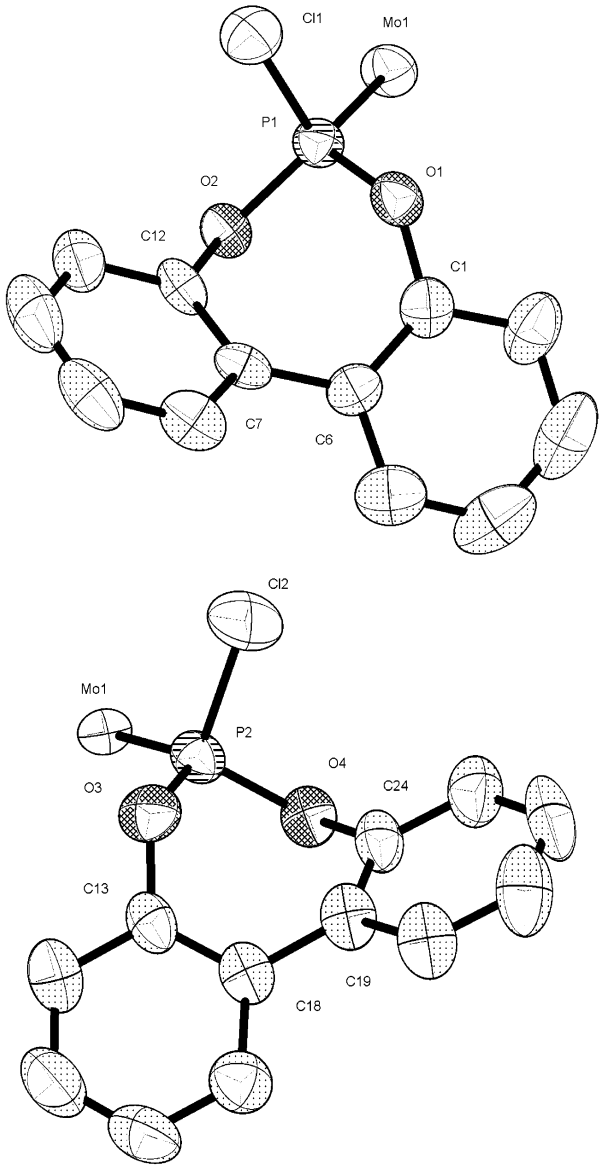

Figure 9. ORTEP rendition of both enantiomers of the phosphepin rings in **1**. Thermal ellipsoids are drawn at the 50% probability level, and hydrogen atoms are omitted for clarity.

The conformations of the seven-membered phosphepin rings **1**−**4** are defined by the angles between the least-squares planes through O1, P1, and O2 (plane 1), through O1, C1, and C6 (plane 2) and through O2, C12, and C7 (plane 3). These angles are summarized in Table 5 and are similar for all of the phosphepin ligands in **1**−**4**, with the angles between plane 1 and either plane 2 or plane 3 being between 55.3 and 62.4° and the angles between planes 2 and 3 being between 45.9 and 48.5°. This narrow range of interplanar angles indicates that the phosphepin rings have a strongly preferred conformation that is not significantly affected by either hydrogen-bonding or crystal-packing forces.

(33) Gray, G. M.; Fish, F. P.; Srivastava, D. K.; Varshney, A.; van der Woerd, M. J.; Ealick, S. E. *J. Organomet. Chem.* **1990**, *385*, 49.

The most interesting aspect of the conformation of the phosphepin ligands in **1**−**4** is that the twist of the 2,2′-biphenoxy groups causes each of the ligands to be chiral and the complexes, which contain two ligands, to be diastereomeric. Figure 9 shows a rendition of both enantiomers of the phosphepin rings in **1**. The chirality of the ligands can be determined from the torsion angles about the C−O bonds of the 2,2′-biphenoxy groups, given in Table 4. The conformation of the phosphepin ring requires the torsion angles about the two C−O bonds to have the same sign, and the similar conformations of the phosphepin ligands requires the torsion angles to have approximately the same magnitudes. When both ligands in a complex have the same signs for the C−O torsion angles, as is the case for **2**−**4**, the complex is the *R***R**/*S***S** diastereomer.[32] In contrast, when the torsion angles for the C−O bonds of the two ligands have opposite signs, as is the case for **1**, the complex is the *R***S** diastereomer. It is interesting that complexes **2**−**4** crystallize in centrosymmetric space groups with both the *R***R** and *S***S** enantiomers present in the crystal while complex **1**, which is the meso diastereomer (*R***S** configuration), crystallizes in a noncentrosymmetric $P2_12_12_1$ space group. This is counterintuitive and demonstrates the importance of crystal-packing forces in the determination of the space groups of crystals. It is important to note that, because the [1,3,2]dioxaphosphepin groups of all of the complexes racemize rapidly in solution, the observation of a particular diastereomer in the solid state does not necessarily reflect the distribution of diastereomers in solution.

Conclusions

The reactions of *cis*-$Mo(CO)_4(2,2'\text{-}C_{12}H_8O_2PCl)_2$ (**1**) with HXR (X = NH, O, S; R = alkyl, aryl) nucleophiles in the presence of nitrogen bases yield both the desired disubstituted products *cis*-$Mo(CO)_4(2,2'\text{-}C_{12}H_8O_2PXR)_2$ and the unexpected hydrolysis products $[R_3NH][cis\text{-}Mo(CO)_4(2,2'\text{-}C_{12}H_8O_2PXR)(2,2'\text{-}C_{12}H_8O_2PO)]$. The relative yields of the two products depend on the amount of water that is present in reactions, with excess water giving exclusively the hydrolysis product. Although NMR studies indicate that the *R** and *S** enantiomers of these ligands interconvert rapidly in solution, the use of bulkier biaryl groups with fixed conformations should allow the generation of unique diastereomeric complexes. The ability to cleanly generate the hydrolysis product should allow diastereomeric complexes with chemically inequivalent phosphepin ligands to be prepared in high yields. The use of the appropriate nucleophiles will allow the ligands to interact via hydrogen-bonding interactions, which could generate further asymmetry in the complexes in both the solution and solid states.

Acknowledgment. We thank the NSF-REU Summer Research Program (Grant No. CHE-9820282) at UAB for funding of part of this research. J.M.B. thanks the Chemistry Department of the University of Alabama at Birmingham for a graduate teaching assistantship. H.B. thanks the University of Montevallo for a sabbatical semester.

Supporting Information Available: Tables giving experimental data for the crystallographic studies, bond distances, bond angles, positional parameters, anisotropic thermal coordinates, and hydrogen atom coordinates for compounds **1**−**4**. This material is available free of charge via the Internet at http://pubs.acs.org.

OM030411Z